Electronic Supplementary Material (ESI) for Molecular Systems Design & Engineering.

3D-Printed, Configurable, Paper-based, Autonomous Multi-Organ-on-Paper Platforms

Hongbin Li †[a, b] Feng Cheng †[a], Zixuan Wang [a], Wanlu Li [a], Juan Antonio Robledo-Lara [a, c], and Yu Shrike Zhang *[a]

[a] Division of Engineering in Medicine, Brigham and Women's Hospital, Department of Medicine, Harvard Medical School, Cambridge, MA 02139, USA
[b] College of Light Industry and Textile, Qiqihar University, Qiqihar, Heilongjiang 161000, P. R. China
[c] Departamento de Ingeniería Mecatrónica y Eléctrica, Escuela de Ingeniería y Ciencias, Tecnológico de Monterrey, CP78211 San Luis Potosí, San Luis Potosí, Mexico

† Hongbin Li and Feng Cheng contributed equally to this work.
* Corresponding Author: yszhang@research.bwh.harvard.edu (Y.S.Z.)

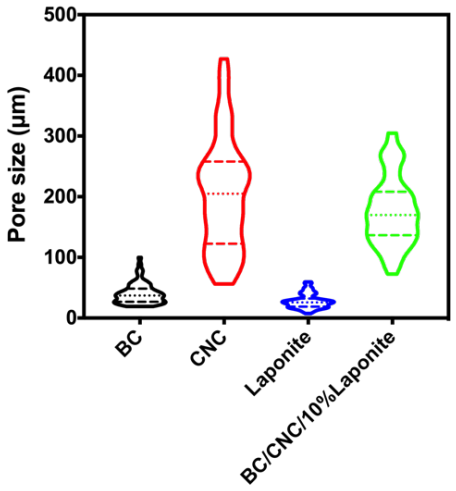

Fig. S1. Quantification of the pore sizes of the BC (1 w/v%), CNC (3 w/v%), Laponite (10 w/v%), as well as the mixture of BC (1 w/v%) and CNC (3 w/v%) with Laponite (10 w/v%) after freeze-drying, which were obtained from the SEM images.

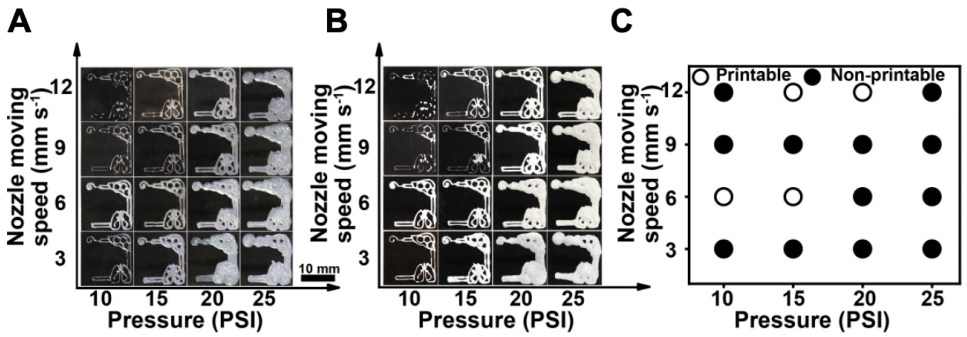

Fig. S2. Printability of the BC/CNC/Laponite inks. (A, B) Photographs showing the ink formulation of 1 w/v% BC and 3 w/v% CNC supplemented with 10 w/v% Laponite extruded at different extrusion pressures (10-25 PSI) and nozzle moving speeds (3-12 mm s^{-1}), before and after freeze-drying, respectively. (E) Corresponding printability mapping. Open circles: printable; filled circles: non-printable.

Fig. S3. Photographs showing the siphon effect of the liver-lung multi-organ-on-paper platform with three layers of printed structure at the 4 mm of height of the medium reservoir with 3 mm in diameter of the evaporation opening of volatilization chamber at different time points.

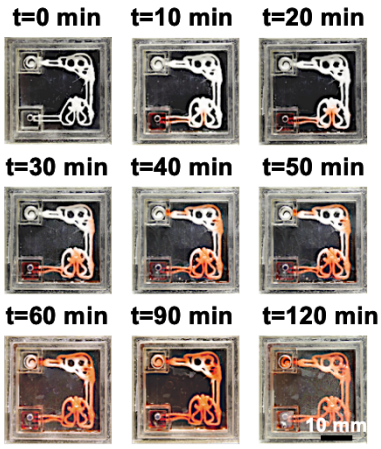

Fig. S4. Photographs showing the siphon effect of the liver-lung multi-organ-on-paper platform with three layers of printed structure at the 6 mm of height of the medium reservoir with 3 mm in diameter of the evaporation opening of volatilization chamber at different time points.

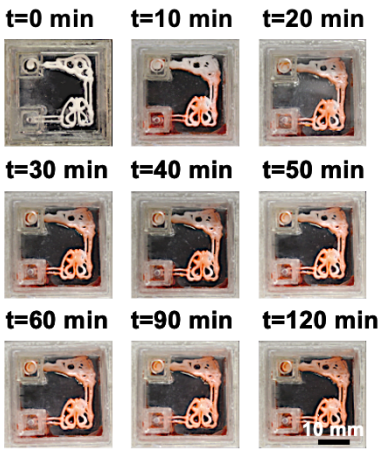

Fig. S5. Photographs showing the siphon effect of the liver-lung multi-organ-on-paper platform with three layers of printed structure at the 10 mm of height of the medium reservoir with 3 mm in diameter of the evaporation opening of volatilization chamber at different time points.

Fig. S6. Photographs showing the siphon effect of the liver-lung multi-organ-on-paper platform with three layers of printed structure at the 6 mm of height of the medium reservoir with 2 mm in diameter of the evaporation opening of volatilization chamber at different time points.

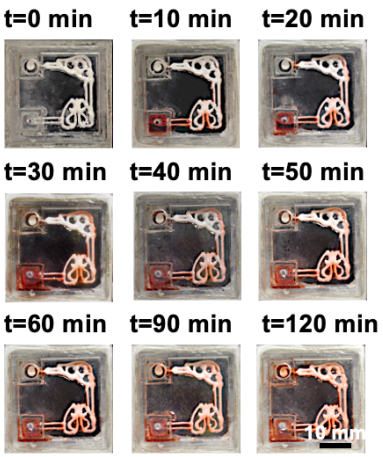

Fig. S7. Photographs showing the siphon effect of the liver-lung multi-organ-on-paper platform with three layers of printed structure at the 6 mm of height of the medium reservoir with 4 mm in diameter of the evaporation opening of the volatilization chamber at different time points.

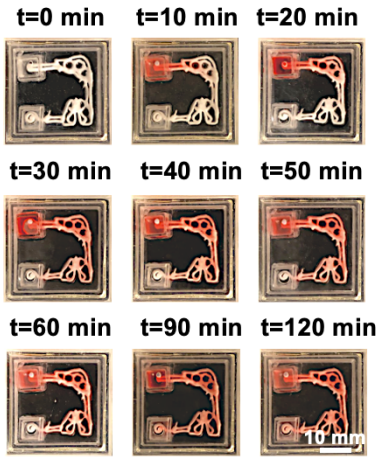

Fig. S8. Photographs showing the siphon effect of the liver-lung multi-organ-on-paper platform with five layers of printed structure at the 6 mm of height of the medium reservoir with 3 mm in diameter of the evaporation opening of the volatilization chamber at different time points.

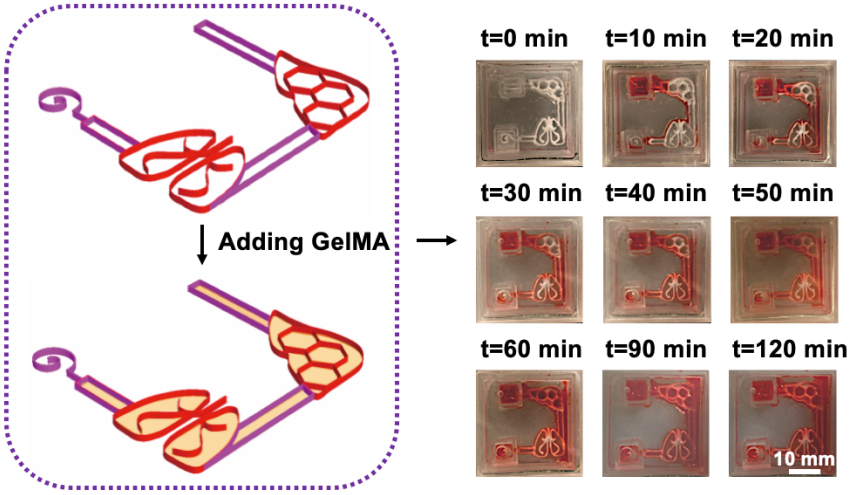

Fig. S9. Photographs showing the siphon effect of the liver-lung multi-organ-on-paper platform with three layers of printed structure loaded with the GelMA hydrogel at the 6 mm of height of the medium reservoir with 3 mm in diameter of the evaporation opening of volatilization chamber at different time points.

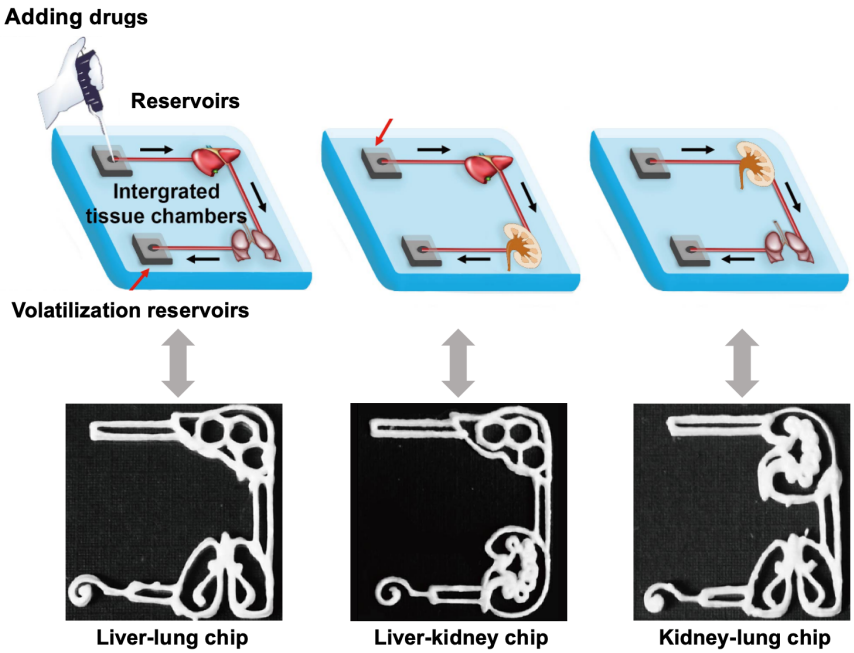

Fig. S10. Schematic diagram showing the operation principle of the multi-organ-on-a-chip platforms.

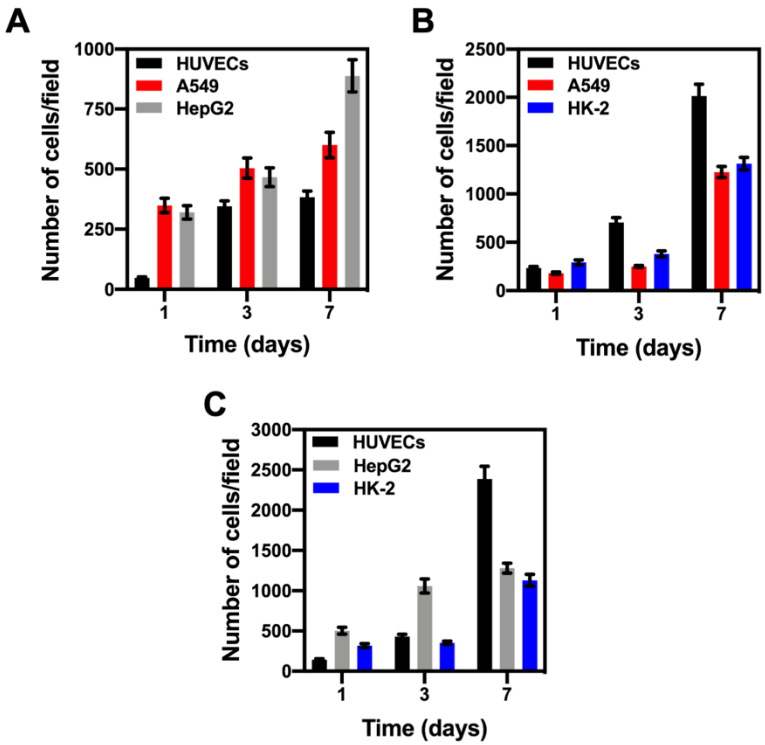

Fig. S11. Quantitative analyses of the numbers of HepG2 cells, A549 cells, and HUVECs at 1, 3, and 7 days of culture in (A) the liver-lung chip, (B) the kidney-lung chip, and (C) the liver-kidney chip. The area of the field in the images was 1.21 mm^2.

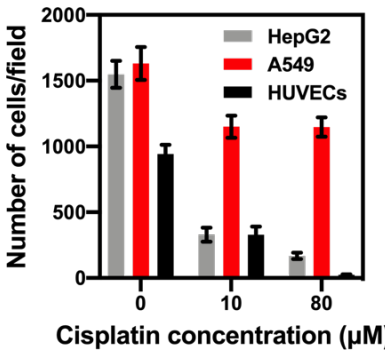

Fig. S12. Quantitative analyses of the numbers of HepG2 cells, A549 cells, and HUVECs cells treated with different concentrations of cisplatin (0-80 μM) in the liver-lung chips. The area of the field in the image was 1.21 mm^2.

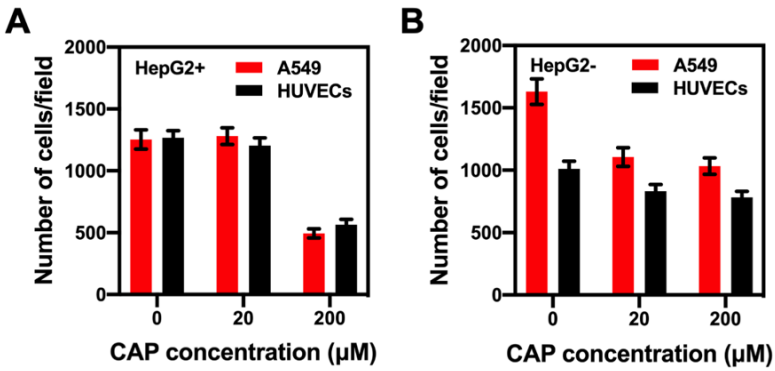

Fig. S13. Quantitative analyses of the numbers of A549 cells and HUVECs cells treated with different concentration of CAP (0-200 μM) metabolized or not metabolized by HepG2 cells in the liver-lung chips. (A) CAP metabolized by HepG2 cells. (B) CAP not metabolized by HepG2 cells. The area of the field in the images was 1.21 mm^2.